Fibers and Polymers 2017, Vol.18, No.12, 2368-2378
DOI 10.1007/s12221-017-7631-8

ISSN 1229-9197 (print version)
ISSN 1875-0052 (electronic version)

Prediction of Diameter in Blended Nanofibers of Polycaprolactone-Gelatin Using ANN and RSM

Tahere Khatti[1], Hossein Naderi-Manesh[2]*, and Seyed Mehdi Kalantar[3]

[1]*Department of Nanobiotechnology, Faculty of Biological Sciences, Tarbiat Modares University, Tehran 14115-111, Iran*
[2]*Department of Biophysics/Nanobiotechnology, Faculty of Biological Sciences, Tarbiat Modares University, Tehran 14115-111, Iran*
[3]*Department of Genetics, Research and Clinical Center for Infertility, Shahid Sadoughi University of Medical Sciences, Yazd 89195-999, Iran*

(Received July 25, 2017; Revised October 21, 2017; Accepted October 24, 2017)

Abstract: Fabrication of nanofibers with a defined diameter is a primary purpose of the electrospinning process. The diameter of nanofiber is directly related to its individual features, such as mechanical property and porosity. The motivation to conduct the current study was to explore the diameter of hybrid nanofibers of polycaprolactone-gelatin (PCL-GT) as one of the most attractive scaffolds employed in various research fields, such as tissue engineering and industrial fields. We have developed two predictive models describing the electrospinning process of PCL-GT using response surface methodology (RSM) and artificial neural network (ANN). The effect of 4 variables on diameter was analyzed, including total polymer concentration, ratio of PCL to Gel, voltage, and tip-to-collector distance. The individual and interactive effects of the mentioned factors were analyzed using RSM. The total polymer concentration had the most significant individual effect on the diameter of PCL-Gel nanofiber, whereas the other three factors showed less strong individual effects, although, the interactive effects of these factors were more remarkable. It was demonstrated that both models, especially the ANN model, could accurately predict the diameter of PCL-GT nanofiber (regression coefficient > 0.92, mean absolute percentage error < 5.7). The represented predictive models could facilitate construction of electrospun nanofibers from PCL-Gel with well-controlled diameter required for any intended purpose.

Keywords: Electrospinning, Nanofiber, Artificial neural networks, Response surface methodology, Polycaprolactone, Gelatin

Introduction

Tissue engineering generally refers to assembling scaffolds, cells, and biological molecules aiming to produce functional tissues [1,2]. Biocompatible and appropriate scaffold as an essential component of tissue engineering is mostly fabricated using various types of polymers [3]. Polymers in aspect of origin comprise two types, which are synthetic and natural polymers. Each type has its specific characteristics which made it desirable for particular applications [4,5]. Naturally occurring polymers such as cellulose [6,7], silk fibroin [8], and gelatin [9] are water based and consequently have high cell affinity along with poor mechanical properties. On the other hand, synthetic polymers are highly hydrophobic without cell recognition site, although these polymers have acceptable mechanical properties [10,11]. Polymer blending, especially blending synthetic and natural polymers, is extensively utilized in scaffold fabrication, in order to achieve desirable cell adhesion, degradation rate, and mechanical properties [4,12].

Polycaprolactone (PCL) is one of the most used synthetic polymers in the biomedical field [13]. PCL is a biodegradable hydrophobic semi crystalline polymer, and its merits over other biopolymers are ease of synthesis, inexpensive production, tailorable mechanical properties, flexibility in surface modification, and long-term degradation time [14]. On the other hand, gelatin that is obtained from hydrolysis of collagen comprises a set of distinct properties, such as hydrophilic nature, high cell affinity, poor mechanical properties, good biodegradability, and low cost [15]. Blending of PCL and gelatin could relatively cover the weaknesses of both polymers [16]. As reported in the literature, polycaprolactone-gelatin (PCL-GT) composite has been applied in wound healing [17], tissue engineering of nerves [18], muscle [19], teeth [20], and cardiovascular tissue [21], and in the fields of cancer [22] and stem cell research [23].

Among the most practical and efficient structures utilized in the biomedical field, particularly in tissue engineering, are nano and microfiber. These fibers could nobly mimic the structure of extracellular matrix (ECM) if designed accurately [24]. Fiber diameter, porosity, and mechanical properties are some of key parameters in the design of an intended scaffold.

Although, there are several methods for fabrication of nanofibers, electrospinning has emerged as the most commonly used technique for polymeric nano and microfiber production [25]. In this method, by exploiting an electric force, polymer solution or melt that is extruded from a syringe is continuously drawn until nanofiber is produced. Some of the advantages of the above- mentioned technique include ease of use, versatility, low cost, and fiber fabrication from a wide variety of polymers [26,27]. There are 4 sets of parameters

*Corresponding author: naderman@modares.ac.ir

influencing electrospun nanofiber properties, including polymer characteristic (molecular weight, solubility), polymer solution factors (such as viscosity, conductivity, and concentration), processing parameters (including voltage, tip-to-collector distance, and feed rate), and ambient condition (temperature, humidity) [28]. These parameters affect the electrospinning process both alone and in combination with other parameters. Formulation and prediction of the factors that affect the output of the electrospinning process have considerable importance in the fabrication of any desirable nanofibrous scaffold.

Modeling techniques such as RSM and ANN assist in determining the complicated patterns of variables that affect a process. Such modeling techniques facilitate understanding a process and decrease the cost and time of performing experiments. RSM is a statistical method, which explores the quantitative relationship between independent variables and output of a process. RSM is capable of presenting a mathematical equation to demonstrate clearly the relationship of variables and response. Furthermore, this technique could be an efficient tool for optimization of numerous types of processes. The basic principles of RSM consist of fitting an empirical model to the experimental data, applying polynomial functions. The initial step of RSM is selection of more effective variables and design of experiments, which is performed by various methods such as Taguchi, Box-Behnken design, central composite design, and more. After conducting the designed experiment, the resultant responses are mathematically and statistically analyzed to achieve an acceptable model fit. Verification of the fitness of the model and optimization study are the last steps of RSM [29,30].

A further technique, which is broadly applied as a predictive modeling tool to study different kinds of processes, is artificial neural network (ANN), which is inspired from the natural nervous system [31]. This powerful network is a collection of artificial neurons in different layers that are interconnected for processing input information, with the aim of obtaining an output. In a simple artificial neuron, the input is multiplied by weight (strength of signal) and then processed by transfer function of neuron to estimate the output. Training, validating, and testing are necessary steps of ANN modeling. Training is performed using multiple input-response data points in order to approximate the relationship between the datasets. The next two steps, validation and testing, are critical stages for verification of the created network performance [32].

In recent years, due to the importance of nanofibers in various scientific fields, especially biomedicine, researchers have paid more attention to modeling the electrospinning process. Most recent modeling studies have focused on the effect of processing variables on fiber diameter and morphology. Polyethylene oxide [33], polymethyl methacrylate [34,35], polyurethane [36], polyacrylonitrile [37-39], Gelatin [40] and polycaprolactone [41] are some of investigated polymers modeled by ANN and RSM to predict fiber diameter. In some other studies, the electrospinning process was modeled with the purpose of predicting different characters of nanofibrous scaffold [42]. For instance, mechanical properties of PCL-GT scaffolds were predicted using a single-layer perceptron ANN [43], or the mechanical features of polycaprolactone/nano hydroxyl apatite [44] were studied using RSM modeling.

In the present paper, we studied the influence of multiple factors affecting the electrospinning process of PCL-GT nanofiber diameter. The considered parameters included total concentration of polymer solution, volume ratio of the two polymers, applied voltage, and distance of nozzle to collector. Using central composite design method, thirty experiments were designed in order to explore the effect of the mentioned variables. PCL-Gel nanofibers were fabricated in the thirty experimental conditions and then their diameters were measured from SEM images. The obtained information was applied as the input data for modeling. The mentioned factors and their interactions were modeled by applying ANN and RSM methods. Consequently, the results obtained from the two models were compared in terms of prediction accuracy.

Experimental

Materials

Polycaprolactone (PCL, Mw=80,000) and gelatin (GT) type A (300 Bloom) from porcine skin were purchased from Sigma-Aldrich. Trifluoroethanol (TFE) and acetic acid were obtained from Merck.

Preparation of Polymer Solution

PCL and GT were dispersed in TFE separately at concentrations of 5 %, 6 %, 7 %, 8 %, and 9 % (w/v). Each solution was stirred for about 3 hours. Before the electrospinning process, the two polymer solutions were mixed and a tiny amount (<0.3 %) of acetic acid was added in order to achieve a miscible and transparent solution [45].

Electrospinning

Electrospun PCL-GT scaffolds were fabricated using an electrospinning device (Nanoazma Co., Tehran, Iran). The prepared solution was extruded from a 10 m*l* syringe attached to a 21 G blunted needle. The fibers were collected by a cylindrical collector (17 cm×5 cm) on an aluminum foil. The feed rate was 0.5 m*l*/h and a speed of 300 RPM was selected for collecting the random fibers. The electrospinning was carried out at 25 ^{o}C. After electrospinning, the fibrous mats were dried for 48 hours. The experimental set-up used for electrospinning of PCL-Gel nanofiber is shown in Figure 1.

Morphological Characterization

The morphology of electrospun fibers was explored via a

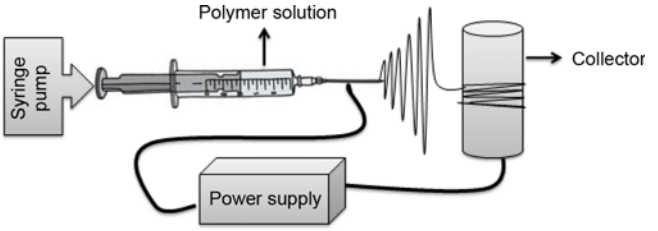

Figure 1. Electrospinning setup utilized for fabrication of PCL-Gel nanofiber.

scanning electron microscope (SEM; TESCAN, Brno, Czech Republic) at an accelerating voltage of 30 kV under 3000x magnification after sputter coating with gold using a sputter coater. Applying Image J software (v. 2), the diameter of 100 fibers in each SEM micrograph was measured and average fiber diameter was calculated. To analyze the distribution of fibers' diameters, SPSS software (v. 15, SPSS Inc., Chicago) was applied.

Experimental Design

Central composite design (CCD) was employed to assess statistically the effective variables on the diameter of electrospun nanofibers [46]. From the literature, we have identified the most 4 important factors affecting the diameter of PCL-GT nanofiber, which comprise total polymer concentration, weight ratio of PCL-GT, voltage, and distance between nozzle and collector. The range of the variables and their levels was determined by trial experiments, which indicated the attainable limits for nanofiber formation. The chosen variables and their levels are shown in Table 1.

In order to construct the design, the coded values of the corresponding actual factors were determined by the following equation:

$$Y_i = \frac{y_i - y_0}{\Delta y_i} \quad (1)$$

where Y_i is the coded value of the variable, y_i is the actual value of the variable at the center point, and Δy_i is the step change of the variable.

The CCD included 30 experimental trials, with 6 experiments to replicate the center point. The central values in our study include 14 % (w/v) for total concentration, 50:50 (v/v) for polymer ratio, 15 (kV) for applied voltage, and 12 cm for tip-to-collector distance.

To predict the response, estimation of coefficients in a mathematical model was performed using Design-Expert software (v. 7.0.0 trial).

Table 1. Actual and coded values of the selected parameters

	Coded value				
	-2	-1	0	1	2
A: Polymer concentration (%w/v)	10	12	14	16	18
B: Weight ratio of PCL: gelatin	20:80	35:65	50:50	65:35	80:20
C: Voltage (kV)	9	12	15	18	21
D: Tip-to-collector distance (cm)	8	10	12	14	16

Artificial Neural Networks

In this research, a three-layer perceptron feed forward network with two hidden layers and one output layer was used [47]. The number of neurons in the first and second hidden layers was 17 and 7, respectively.

In order to achieve the optimum structure of the network, we inquired different numbers of hidden layer and neurons and compared them via mean squared error (MSE) and linear correlation coefficient (R^2).

The input data, which included the diameter of the resultant nanofiber, was randomly divided into training (70 % of the data), validating (15 % of the data), and testing (15 % of the data). For training, the network back propagation (BP) algorithm in conjugation with scaled conjugate gradient (SCG) method was selected. Three types of activation function were used, including hyperbolic tangent sigmoid, logistic sigmoid, and linear functions for the first, second, and third layers of the network, respectively.

All raw data were normalized before ANN modeling. The analysis of the data was carried out using the ANN toolbox of MATLAB mathematical software (v. 7.0).

Comparison of the performance of ANN and RSM models was accomplished by calculation of linear correlation coefficient (R^2) and mean absolute percentage error according to equation (2) and (3):

$$R^2 = 1 - \frac{\sum_{i=1}^{n}(x_i - \hat{x}_i)^2}{\sum_{i=1}^{n}(x_i - \overline{x}_i)^2} \quad (2)$$

$$\text{Mean absolute error} = \frac{1}{n}\sum_{i=1}^{n}\frac{(x_i - \hat{x}_i)}{\hat{x}_i} \quad (3)$$

where $x, \hat{x}$ and $\overline{x}$ are the measured, predicted, and average value of fiber diameter and n represents the number of experiments.

Results and Disscusion

RSM Study

After preliminary screening to obtain more effective variables, the appropriate range of input value was determined and design of experiment was carried out based on the CCD method (Tables 1 and 2). Thirty experiments acquired by the above-mentioned technique were conducted and the diameter of produced nanofiber was explored using SEM. Figure 2 indicated the morphology of some obtained PCL-GT nanofiber and the diameter distribution.

We have utilized multiple regression analysis to detect accurately the best statistical model fitting all of the design

Table 2. The experimental conditions designed by central composite method and obtained responses

Run	Coded value of A	Coded value of B	Coded value of C	Coded value of D	Response fiber diameter (nm)
1	1	1	1	-1	170
2	-1	1	-1	-1	156
3	0	0	0	0	119
4	-1	-1	1	-1	171
5	0	0	0	0	113
6	0	0	0	0	119
7	0	0	0	0	119
8	-1	1	1	1	147
9	0	0	-2	0	142
10	1	1	-1	1	164
11	-1	-1	-1	-1	147
12	0	2	0	0	137
13	0	0	0	0	119
14	-2	0	0	0	140
15	0	-2	0	0	149
16	1	-1	-1	-1	153
17	1	-1	1	-1	148
18	0	0	0	0	121
19	2	0	0	0	266
20	0	0	0	2	148
21	1	1	-1	-1	135
22	-1	-1	1	1	187
23	1	1	-1	1	184
24	0	0	2	0	137
25	-1	-1	1	-1	141
26	1	1	1	1	167
27	-1	-1	1	1	148
28	1	1	-1	-1	179
29	-1	-1	-1	1	137
30	0	0	0	-2	149

(A) polymer concentration, (B) weight ratio PCL: GT, (C) applied voltage, and (D) tip to collector distance.

points. The cubic model was consequently found to be the most appropriate model for analyzing the diameter of PCL-GT fiber.

Thereupon, statistical analysis of the obtained responses was carried out. Analysis of variance (ANOVA) was employed to discover clearly that a relationship existed within the electrospinning process of PCL-GT. As can be seen in the ANOVA table (Table 3), 10 terms had a P-value less than 0.05, which meant that these terms had a significant effect on the diameter of PCL-GT nanofibers. Additional terms with P-value greater than 0.05 were eliminated to improve the model.

The model P-value of less than 0.0001 obviously revealed the significance of the response surface-reduced cubic model. Furthermore, lack of fit term was non-significant (0.2552) at 95 % confidence level, which corroborated that the proposed model represented the data satisfactorily. Accordingly, the following regression equation was obtained from the ANOVA, aiming to approximate the diameter of PCL-GT electrospun nanofiber:

$$R = 116.83 - 4.37CD + 21.52A^2 + 6.52B^2 + 5.65C^2 + 7.90D^2 + 8.63ABC - 6.62ABD + 5.50A^2B - 5A^2C + 7.46A^3 \quad (4)$$

where R, A, B, C, D are the average diameter of PCL-GT fibers, coded forms of total polymer concentration, polymer volume ratio, voltage, and tip-to-collector distance, respectively.

In order to check the adequacy of the constructed model, R-squared, adjusted R-squared, and coefficient of variation (CV) were calculated, and were equal to 0.95, 0.92, and 5.4, respectively. The high value of R^2 and the small difference between R^2 and adj-R^2 implied that the developed model accurately represented the system and could be used to navigate the design space. On the other hand, the small values of CV (<10), which is a measure expressing standard deviation as a percentage of the mean, showed the good reproducibility of the model.

To understand better the effect of the variables, we have utilized some graphs to describe this complex relationship. Figure 3(a) illustrated the main effect of the perused variables on the fiber diameter, which was acquired at the mean point of other parameters. As can be seen in Figure 3(a), small variations in total polymer concentration have a drastic effect on the response, especially in the range of 14 % (w/v) to 18 % (w/v). Thus, according to the plots of Figure 3, the most important factor affected the diameter of PCL-Gel nanofiber is the total polymer concentration. This result is in agreement with previous reports clarifying that an increase in polymer concentration will lead to greater fiber diameter via an increase of viscoelastic force [37,48]. Less strong correlation was observed for the remaining three parameters (Figures 3(b), (c), (d)). Concave dependence was observed for the PCL-GT ratio (Figure 3(b)), voltage (Figure 3(c)), and distance (Figure 3(d)), which demonstrated that there was a threshold limit at which the decreasing effect converted to an increasing effect. In other words, in a certain area of the variable range, upon increasing the factor value the diameter decreased, and in an alternate area there was an inverse effect. Interestingly, PCL concentration and Gel concentration have a similar effect on the diameter of PCL-Gel when the total concentration is constant as well as voltage and tip-to- collector distance (Figure 3(b)). In other words, when the total polymer concentration is constant, by altering the ratio of PCL to Gel, no sensible change of diameter is occurred. It is worth mentioning that these main

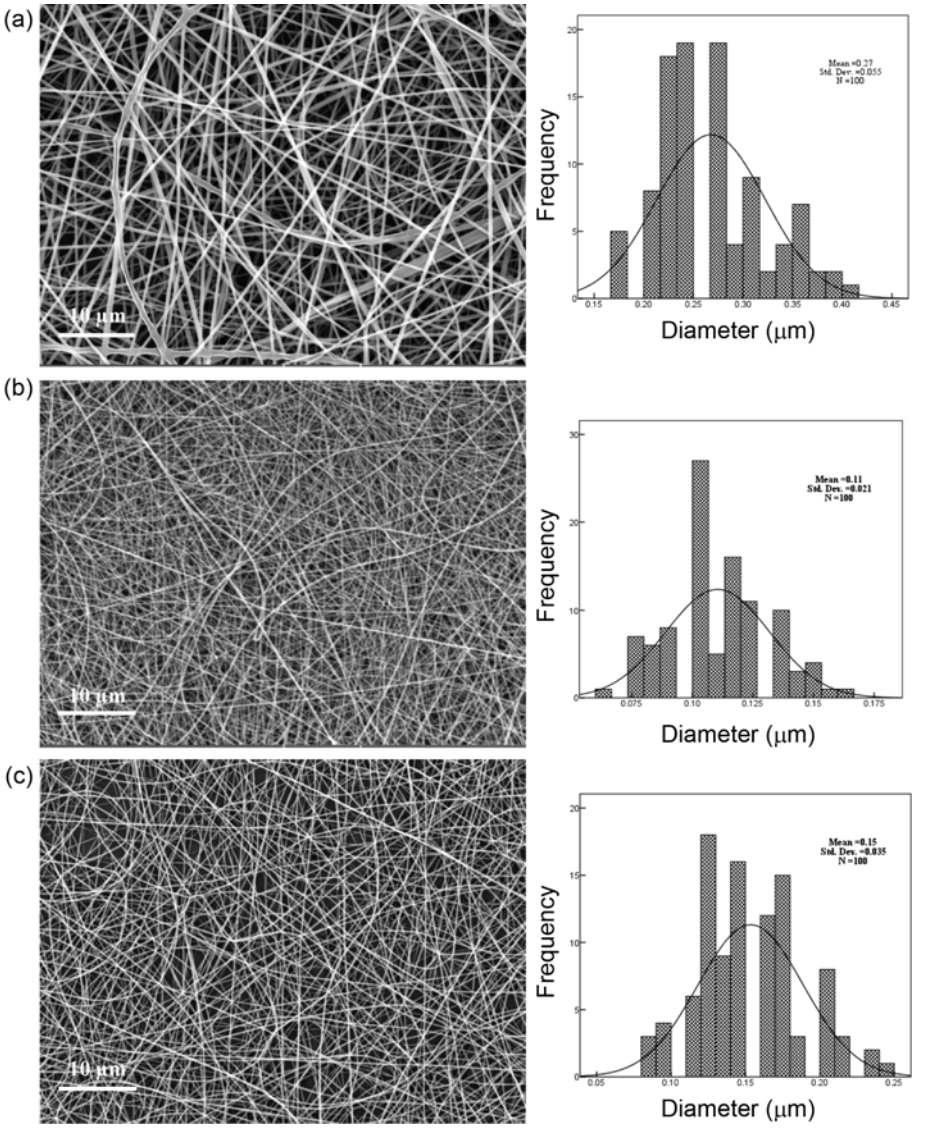

Figure 2. SEM micrograph of electrospun PCL/GT nanofibers and the diameter distribution (a) nanofiber from experiment 19, (b) nanofiber from experiment 5, and (c) nanofiber from experiment 10 indicated in Table 2.

effects were measured without considering the interaction of variables. For exploration of the potential relationship between the variables, contour plot and 3D surface plot were represented. The simultaneous effect of total polymer concentration with PCL-GT ratio and voltage is shown in Figures 4(a) and (b), respectively. As can be seen in Figure 4(a), contour levels reveal a peak centered near 14 % (w/v) of concentration and 50:50 polymer ratio. The diameter in this peak region is near 127 nm. Moving away from the center, the diameter will increase. Similarly, the two alternate contour plots had a center area at the midpoint of the variable rang, which is the area of minimum diameter. The response is increased around the center (Figures 4(b) and (c)).

3D surface plot can also be used to explore the potential relationship among the three variables. This plot represents a 3-dimensional view of the surface and provides a clear concept of the response surface. The 3D surface plot of all studied variables is illustrated in Figures 5(a), (b), and (c).

Optimization Study

Response surface methodology is generally used to find a favorite location in the design space, in the other words, to perform an optimization study. In an optimization study, the goal is to attain a minimum, a maximum, or a special stationary area in the design space. In the present investigation, we optimized the variables to reach a minimum response of nanofiber. Among the suggested solutions represented by the

Table 3. Analysis of variance (ANOVA) for response surface cubic model of PCL/GT fiber diameter

Source	Sum of squares	DF	Mean square	F-value	Prob. > F
Model	24756.03	10	2475.60	37.73	< 0.0001[a]
CD	306.25	1	306.25	4.67	0.0437[a]
A^2	12703.44	1	12703.44	193.61	< 0.0001[a]
B^2	1166.30	1	1166.30	17.78	0.0005[a]
C^2	874.30	1	874.30	13.32	0.0017[a]
D^2	1710.01	1	1710.01	26.06	<0.0001[a]
ABC	1190.25	1	1190.25	18.14	0.0004[a]
ABD	702.25	1	702.25	10.70	0.0040[a]
A^2B	484.00	1	484.00	7.38	0.0137[a]
A^2C	400.00	1	400.00	6.10	0.0232[a]
A^3	8010.25	1	8010.25	122.08	<0.0001[a]
Lack of fit	1045.83	14	74.70	1.86	0.2552[b]
Pure error	200.83	5	40.17		

[a]Significant at 95 % confident interval and [b]not significant at 95 % confident interval.

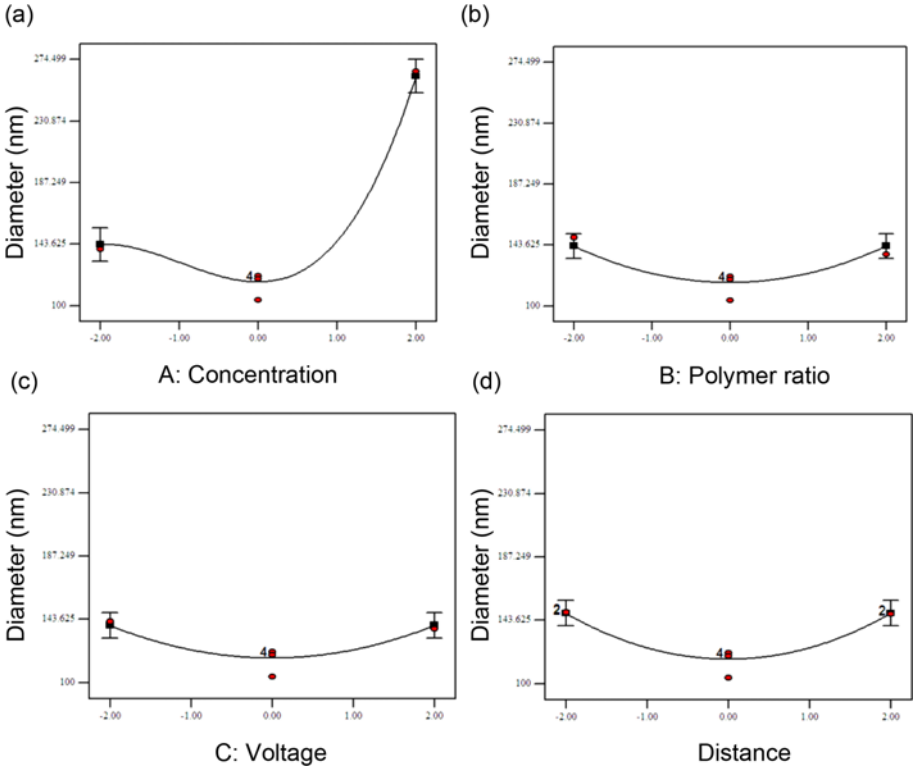

Figure 3. Main effects of the studied variables on PCL/GT fiber diameter based on coded values; (a) polymer concentration, (b) polymer ratio, (c) voltage, and (d) tip-to-collector distance.

software, the most desirable condition for gaining a minimum was at the midpoint of factors, specifically at a concentration of 14 % (w/v), ratio of 50:50, voltage of 15 (kV), and distance of 12 (cm). The predicted diameter at the above- mentioned experimental condition was 116 nm. The experimental value achieved in this situation was 120 nm, which was in a good agreement with the corresponding predicted value. Figure 5(d) shows the obtained model for desirability plotted in 2D and 3D views for an optimum voltage of 15 (kV) and distance of 12 (cm).

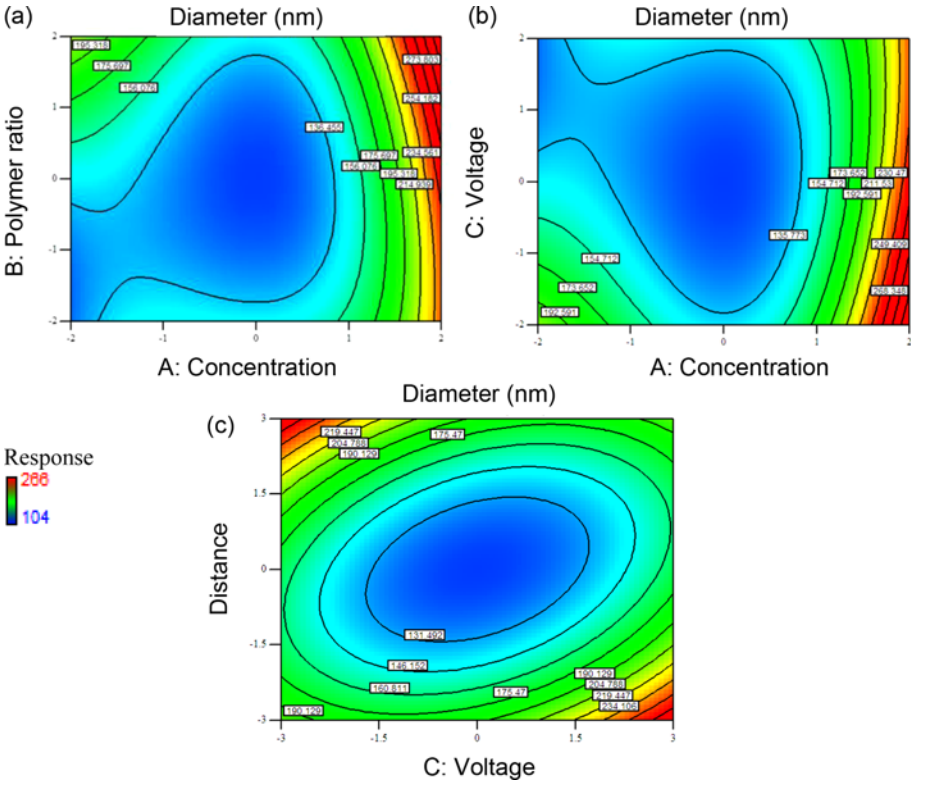

Figure 4. Contour plots of variables for diameter: (a) concentration vs. polymer ratio, (b) concentration vs. voltage, (c) voltage vs. distance, when other variables are at the mean point.

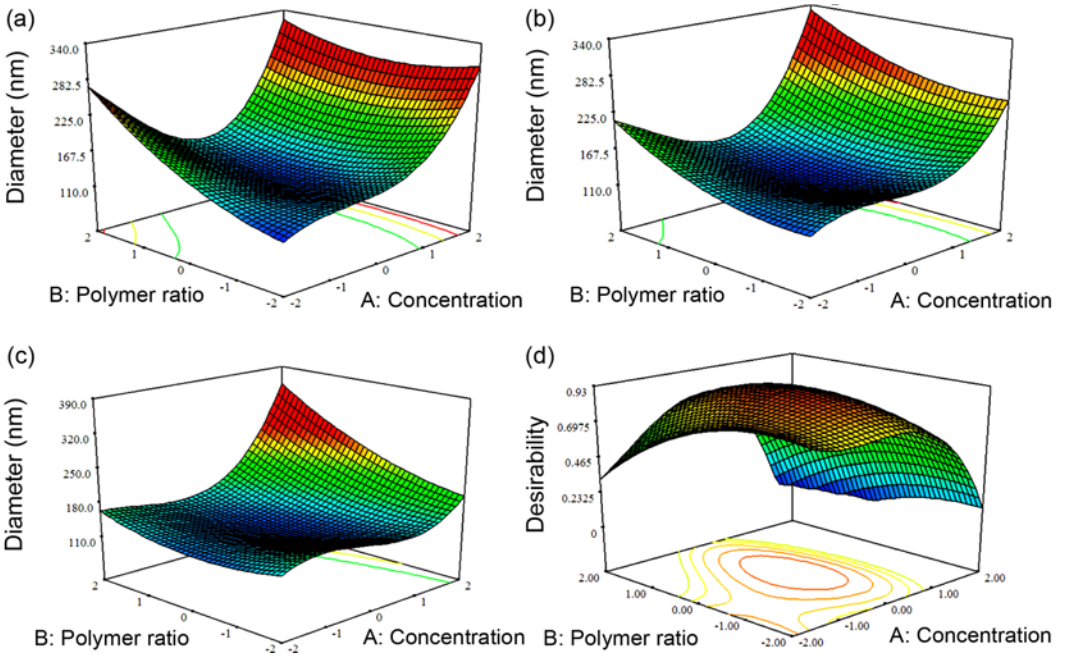

Figure 5. 3-Dimentional surface plot. The interaction of three variables including concentration, polymer ratio and voltage has represented by three 3-D surface plot; (a) plot obtained at voltage of 9 (kV), (b) plot obtained at voltage of 15 (kV) and (c) plot obtained at voltage of 21 (kV), and (d) desirability plot for the obtained mathematical model in 3D view.

ANN Study

Artificial neural network is mostly applied for predictive non-linear modeling of complex data. Hence, we have applied ANN to predict the diameter of electrospun nanofiber. The input data, which feed into the network, are 4

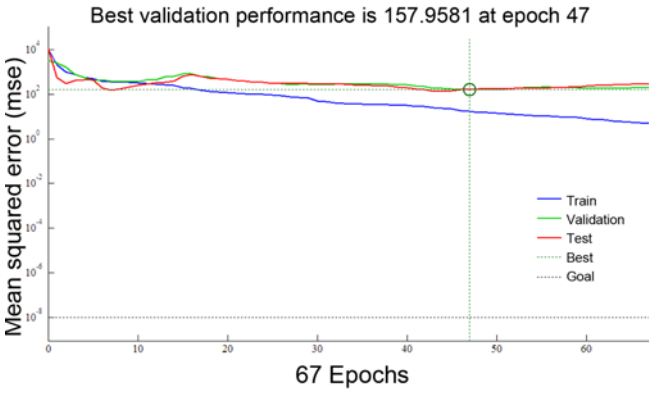

Figure 6. MSE plot with respect to the number of epochs for training, validation, and test samples for the PCL/GT nanofiber diameter.

Table 4. Evaluation of ANN models with different structures

No. of structure	No. of hidden layer	No. of neuron in each layer	R value	MSE
1	1	1	0.32	36
2	1	5	0.51	283
3	1	10	0.83	623
4	1	14	0.72	93
5	1	20	0.68	2119
6	1	24	0.80	66
7	1	30	0.66	3371
8	1	34	0.73	2868
9	2	20-4	0.90	73
10	2	10-14	0.48	1351
11	2	11-13	0.86	35
12	2	2-22	0.68	405
13	2	**17-7**	**0.96**	**157**
14	2	8-16	0.80	407
15	2	7-17	0.79	597
16	2	15-9	0.72	208

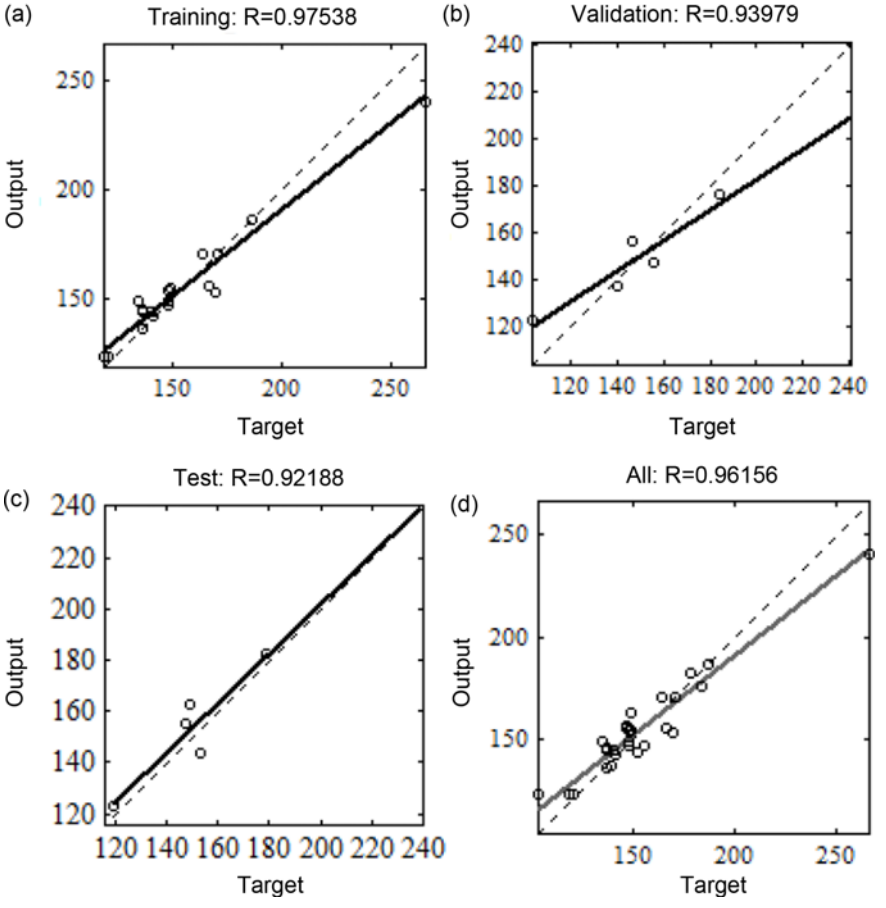

Figure 7. Regression analysis between ANN responses and the experimental results for (a) training, (b) validation, (c) test datasets, and (d) all data.

sets of effective factors on the PCL-GT fiber diameter. The ANN model was created based on MSE (mean squared error) and R value of the datasets of different examined structures of the network (Table 4). The optimum arrangement of ANN in our study was a three-layer perceptron feed forward ANN with 17, 7, and 1 neurons in the first, second, and output layer, respectively. Defining the number of neurons in each layer was done to prevent overfitting, which results from having too many neurons, and underfitting that is due to too few neurons.

In order to train the created network, 30 input-response data points were utilized and the learning process was performed based on scaled conjugate gradient back propagation algorithm. SCG is a supervised learning algorithm for feed-forward neural networks and is a member of the conjugate gradient method [49].

When the training data set is processed through the network while the weights between connections are adjusted, the predicted output value is produced from output nodes. Then, these output values are compared to the real values of outputs and the comparison is subsequently evaluated by calculation of MSE of the training and testing sets. Figure 6 represents the MSE plot of all 30 data sets, which has a descending trend while the network is learning. The best network performance was at MSE equaling 157.95, acquired at epoch 47.

Furthermore, the performance of the trained network was depicted by parity plot, which compares actual data against predicted data (Figure 7). The correlation coefficient is a criterion of how well the obtained model truly represents the actual data. In a perfect correlation, the above-mentioned coefficient is equal to one. According to the represented plots in Figure 7, the R^2 value of all datasets was equal to 0.92, which validated the goodness of fit.

Comparison of RSM and ANN Results

With the purpose of.detecting a more accurate predictive model, ANN and RSM were compared in terms of the linear regression coefficient (R^2) and mean absolute percentage error as summarized in Table 5. R-squared value for ANN and RS models was almost identical and equal to 0.92. Note, however, that the mean absolute percentage error calculated by equation (3) was 4.02 % for the ANN model and 5.76 % for the RS model. Accordingly, both models have a suitable compromise with the actual data, which is revealed in the good performance of the two models. Considering the above-mentioned values, the ANN model surpassed the RSM model to some extent due to lower percentage error. Previous reports on using RSM and ANN to study the electrospinning process have indicated that ANN models frequently had more accurate predictions than RSM, however, in some cases, there was subtle difference between the two techniques' results [34,36,50]. Noteworthily, regardless of accuracy, RSM has some considerable advantages over ANN. The most important benefit of RSM is providing an equation that exhibits all factors' contributions and their interactions. Using this regression model, one can detect insignificant main and interactive terms and thus eliminate them to simplify the relationship. However, ANN technique cannot represent an equation and provides little information about factors' contributions if further analysis has not been done. Moreover, ANN requires more time for computation and greater cost than does the RSM technique.

Table 5. Comparison between experimental and predicted values via RSM and ANN models

Sample	Experimental	Predicted	
		RSM	ANN
1	170	186	169
2	156	159	145
3	119	116	120
4	171	160	164
5	113	116	120
6	119	116	120
7	119	116	120
8	147	145	159
9	142	139	137
10	164	165	163
11	147	144	155
12	137	142	135
13	119	116	120
14	140	143	148
15	149	142	152
16	153	163	154
17	148	144	141
18	121	116	120
19	266	262	261
20	148	148	152
21	135	186	141
22	187	139	184
23	184	165	183
24	137	139	113
25	141	160	142
26	167	164	159
27	148	138	127
28	179	170	179
29	137	139	134
30	149	148	145
R^2 value		0.921	0.921
Mean absolute error (%)		5.76	4.02

Conclusion

The current study aimed to predict the diameter of electrospun PCL-GT nanofiber when small variation in the effective factors of electrospinning had occurred. Applying RSM and ANN modeling methods, our achievement was to predict precisely the diameter of intended polymeric fibers as a function of four electrospinning variables including total concentration, polymer ratio, voltage, and tip-to-collector distance. Both represented models described the system accurately, although the ANN model was slightly more accurate than the RSM. The most effective parameters were total polymer (PCL and GT) concentration. With the help of response surface technique, we defined the contribution of each factor and interaction among them. Through optimization study, we determined the experimental situation in which the diameter was at minimum value. The optimum condition obtained was the same as the center point of design space. Relying on these results, we conclude that ANN and RSM are powerful tools for predicting and formulating effective factnaghors in the electrospinning process. Using these techniques, researchers are able to design electrospinning processes in order to attain a desirable diameter, which is required for certain applications.

References

1. Q. P. Pham, U. Sharma, and A. G. Mikos, *Tissue Eng.*, **12**, 1197 (2006).
2. I. Armentano, M. Dottori, E. Fortunati, S. Mattioli, and J. Kenny, *Polym. Degrad. Stabil.*, **95**, 2126 (2010).
3. C. P. Barnes, S. A. Sell, E. D. Boland, D. G. Simpson, and G. L. Bowlin, *Adv. Drug Deliv. Rev.*, **59**, 1413 (2007).
4. A. Sionkowska, *Prog. Polym. Sci.*, **36**, 1254 (2011).
5. H.-Y. Cheung, K.-T. Lau, T.-P. Lu, and D. Hui, *Compos. Pt. B-Eng.*, **38**, 291 (2007).
6. M. Jawaid and H. A. Khalil, *Carbohydr. Polym.*, **86**, 1 (2011).
7. K. Ohkawa, S. Hayashi, A. Nishida, H. Yamamoto, and J. Ducreux, *Text. Res. J.*, **79**, 1396 (2009).
8. S. H. Kim, Y. S. Nam, T. S. Lee, and W. H. Park, *Polymer*, **35**, 185 (2003).
9. M. Li, M. J. Mondrinos, M. R. Gandhi, F. K. Ko, A. S. Weiss, and P. I. Lelkes, *Biomaterials*, **26**, 5999 (2005).
10. J. D. Kretlow and A. G. Mikos, *Tissue Eng.*, **13**, 927 (2007).
11. S. Hosseinzadeh, M. Mahmoudifard, F. Mohamadyar-Toupkanlou, M. Dodel, A. Hajarizadeh, M. Adabi, and M. Soleimani, *Bioproc. Biosyst. Eng.*, **39**, 1163 (2016).
12. M. G. Cascone, B. Sim, and D. Sandra, *Biomaterials*, **16**, 569 (1995).
13. M. A. Woodruff and D. W. Hutmacher, *Prog. Polym. Sci.*, **35**, 1217 (2010).
14. M. Labet and W. Thielemans, *Chem. Soc. Rev.*, **38**, 3484 (2009).
15. Z.-M. Huang, Y. Zhang, S. Ramakrishna, and C. Lim, *Polymer*, **45**, 5361 (2004).
16. Y. Zhang, H. Ouyang, C. T. Lim, S. Ramakrishna, and Z. M. Huang, *J. Biomed. Mater. Res. Part B: Appl. Biomater.*, **72**, 156 (2005).
17. E. Chong, T. Phan, I. Lim, Y. Zhang, B. Bay, S. Ramakrishna, and C. Lim, *Acta Biomater.*, **3**, 321 (2007).
18. L. Ghasemi-Mobarakeh, M. P. Prabhakaran, M. Morshed, M.-H. Nasr-Esfahani, and S. Ramakrishna, *Biomaterials*, **29**, 4532 (2008).
19. M. S. Kim, I. Jun, Y. M. Shin, W. Jang, S. I. Kim, and H. Shin, *Macromol. Biosci.*, **10**, 91 (2010).
20. X. Yang, F. Yang, X. F. Walboomers, Z. Bian, M. Fan, and J. A. Jansen, *J. Biomed. Mater. Res. Part A*, **93**, 247 (2010).
21. S. Heydarkhan-Hagvall, K. Schenke-Layland, A. P. Dhanasopon, F. Rofail, H. Smith, B. M. Wu, R. Shemin, R. E. Beygui, and W. R. MacLellan, *Biomaterials*, **29**, 2907 (2008).
22. O. Hartman, C. Zhang, E. L. Adams, M. C. Farach-Carson, N. J. Petrelli, B. D. Chase, and J. F. Rabolt, *Biomaterials*, **31**, 5700 (2010).
23. K. Gauthaman, J. R. Venugopal, F. C. Yee, G. S. L. Peh, S. Ramakrishna, and A. Bongso, *J. Cellular Molecul. Med.*, **13**, 3475 (2009).
24. S. Srouji, T. Kizhner, E. Suss-Tobi, E. Livne, and E. Zussman, *J. Mater. Sci.: Mater. Med.*, **19**, 1249 (2008).
25. F. Memarian, M. A. Tehran, and M. Latifi, *J. Ind. Text.*, 1528083716679156 (2016).
26. S. Agarwal, J. H. Wendorff, and A. Greiner, *Polymer*, **49**, 5603 (2008).
27. W. E. Teo and S. Ramakrishna, *Nanotechnology*, **17**, R89 (2006).
28. T. Subbiah, G. Bhat, R. Tock, S. Parameswaran, and S. Ramkumar, *J. Appl. Polym. Sci.*, **96**, 557 (2005).
29. W. Sha and K. Edwards, *Mater. Des.*, **28**, 1747 (2007).
30. M. A. Bezerra, R. E. Santelli, E. P. Oliveira, L. S. Villar, and L. A. Escaleira, *Talanta*, **76**, 965 (2008).
31. H. Brooks and N. Tucker, *Polymer*, **58**, 22 (2015).
32. M. Gevrey, I. Dimopoulos, and S. Lek, *Ecological Modelling*, **160**, 249 (2003).
33. K. Sarkar, M. B. Ghalia, Z. Wu, and S. C. Bose, *J. Mater. Process. Technol.,* **209**, 3156 (2009).
34. H. M. Khanlou, A. Sadollah, B. C. Ang, J. H. Kim, S. Talebian, and A. Ghadimi, *Neural Computing and Applications*, **25**, 767 (2014).
35. M. K. Sadan, H.-J. Ahn, G. Chauhan, and N. Reddy, *Eur. Polym. J.*, **74**, 91 (2016).
36. A. Rabbi, K. Nasouri, H. Bahrambeygi, A. M. Shoushtari, and M. R. Babaei, *Fiber. Polym.*, **13**, 1007 (2012).
37. O. Yördem, M. Papila, and Y. Z. Menceloğlu, *Mater. Des.*, **29**, 34 (2008).
38. S. Gu, J. Ren, and G. Vancso, *Eur. Polym. J.*, **41**, 2559 (2005).

39. K. Nasouri, A. M. Shoushtari, and M. Khamforoush, *Fiber. Polym.*, **14**, 1849 (2013).
40. M. Naghibzadeh and M. Adabi, *Fiber. Polym.*, **15**, 767 (2014).
41. T. Khatti, H. Naderi-Manesh, and S. M. Kalantar, *Neural Computing and Applications*, 1 (2017).
42. Z. Asvar, E. Mirzaei, N. Azarpira, B. Geramizadeh, and M. Fadaie, *J. Mech. Behav. Biomed. Mater.*, **75**, 369 (2017).
43. E. Vatankhah, D. Semnani, M. P. Prabhakaran, M. Tadayon, S. Razavi, and S. Ramakrishna, *Acta Biomater.*, **10**, 709 (2014).
44. A. Doustgani, E. Vasheghani-Farahani, M. Soleimani, and S. Hashemi-Najafabadi, *Compos. Pt. B-Eng.*, **43**, 1830 (2012).
45. B. Feng, H. Tu, H. Yuan, H. Peng, and Y. Zhang, *Biomacromolecules*, **13**, 3917 (2012).
46. W. J. Hill and W. G. Hunter, *Technometrics*, **8**, 571 (1966).
47. M. Mézard and J.-P. Nadal, *J. Phys. A: Math. Gen.*, **22**, 2191 (1989).
48. S. Sukigara, M. Gandhi, J. Ayutsede, M. Micklus, and F. Ko, *Polymer*, **44**, 5721 (2003).
49. M. F. Møller, *Neural Networks*, **6**, 525 (1993).
50. K. Nasouri, H. Bahrambeygi, A. Rabbi, A. M. Shoushtari, and A. Kaflou, *J. Appl. Polym. Sci.*, **126**, 127 (2012).